Development 137, 159-167 (2010) doi:10.1242/dev.041574

A novel regulatory mechanism for Fgf18 signaling involving cysteine-rich FGF receptor (Cfr) and delta-like protein (Dlk)

Yuichiro Miyaoka[1], Minoru Tanaka[2], Toru Imamura[3], Shinji Takada[4,5] and Atsushi Miyajima[1,*]

SUMMARY

Fibroblast growth factors (FGFs) transduce signals through FGF receptors (FGFRs) and have pleiotropic functions. Besides signal-transducing FGFRs, cysteine-rich FGF receptor (Cfr; Glg1) is also known to bind some FGFs, although its physiological functions remain unknown. In this study, we generated *Cfr*-deficient mice and found that some of them die perinatally, and show growth retardation, tail malformation and cleft palate. These phenotypes are strikingly similar to those of *Fgf18*-deficient mice, and we revealed interaction between Cfr and Fgf18 both genetically and physically, suggesting functional cooperation. Consistently, introduction of Cfr facilitated Fgf18-dependent proliferation of Ba/F3 cells expressing Fgfr3c. In addition, we uncovered binding between Cfr and delta-like protein (Dlk), and noticed that *Cfr*-deficient mice are also similar to *Dlk*-transgenic mice, indicating that Cfr and Dlk function in opposite ways. Interestingly, we also found that Dlk interrupts the binding between Cfr and Fgf18. Thus, the Fgf18 signaling pathway seems to be finely tuned by Cfr and Dlk for skeletal development. This study reveals a novel regulatory mechanism for Fgf18 signaling involving Cfr and Dlk.

KEY WORDS: Cysteine-rich FGF receptor (Cfr), Delta-like protein (Dlk), Fibroblast growth factor 18 (Fgf18)

INTRODUCTION

The fibroblast growth factor (FGF) family consists of 22 members in mice and humans, and has pleiotropic roles. Gene targeting studies have clearly demonstrated that some FGFs are indispensable to the development of many organs and tissues, including the limbs, lungs, liver, brain, testes, hair follicles and skeleton (Eswarakumar et al., 2005). FGFs transduce intracellular signals via FGF receptors (FGFRs) with a tyrosine kinase. As there are four genes encoding FGFRs in mice and humans, and Fgfr1, Fgfr2 and Fgfr3 each have two splice variants, the FGFR family consists of seven members. Each FGFR binds a subset of FGFs and transduces signals by forming an active receptor complex (Eswarakumar et al., 2005). Besides FGFRs, there are several FGF-binding molecules that also contribute to FGF signaling. Heparan sulfate proteoglycans (HSPGs) are necessary for the dimerization and activation of FGFRs by FGFs (Spivak-Kroizman et al., 1994; Yayon et al., 1991). Klothos are transmembrane proteins that modify the specificity of FGFRs by forming complexes with them and are indispensable for signaling by the FGFs with endocrine functions: i.e. Fgf19 (Fgf15 – Mouse Genome Informatics), Fgf21 and Fgf23 (Kurosu et al., 2007; Kurosu et al., 2006; Suzuki et al., 2008b; Urakawa et al., 2006). FGFR-like 1 (Fgfrl1), which shares sequence homology with FGFRs in its extracellular domain, but lacks an intracellular tyrosine kinase, is also involved in FGF signaling (Wiedemann and Trueb, 2000). Fgfrl1 seems to be a decoy receptor that negatively regulates FGF signaling (Trueb et al., 2003), and has indispensable roles in the development of the diaphragm (Baertschi et al., 2007). Thus, the modulation of FGF signaling by FGF-binding molecules plays important roles in normal developmental processes.

Cysteine-rich FGF receptor (Cfr; Glg1 – Mouse Genome Informatics) is another non-FGFR FGF-binding molecule, which was identified as a transmembrane molecule with affinity for Fgf1 and Fgf2 (Burrus and Olwin, 1989), and subsequently shown to bind Fgf3 and Fgf4 (Burrus et al., 1992; Kohl et al., 2000). Although Cfr binds FGFs via its large extracellular domain consisting of 16 repeats of an unique motif known as the Cfr repeat, it has no sequence homology with FGFRs and its intracellular domain consists of a short peptide of 13 amino acids without a kinase (Zhou et al., 1997). Thus, Cfr is a unique FGF-binding protein and may play a role in FGF signaling like the other FGF-binding proteins described above; however, its functions remain to be elucidated.

In this study, we identified Cfr as a delta-like protein (Dlk)-binding molecule. Dlk, also known as preadipocyte factor 1 (Pref-1), is a transmembrane protein with six epidermal growth factor (EGF) repeats in its extracellular domain. Dlk has sequence homology with Delta, a ligand for Notch, but lacks the Delta/Serrate/LAG-2 (DSL)-motif required for the activation of Notch. Dlk is abundantly expressed in various embryonic tissues (Smas and Sul, 1993) and we previously identified Dlk as a cell surface marker for hepatoblasts, embryonic hepatic progenitor cells (Tanimizu et al., 2003). *Dlk*-deficient mice show several developmental abnormalities such as perinatal death, growth retardation, skeletal abnormalities, increased amounts of adipose tissue and abnormal B cell development (Moon et al., 2002; Raghunandan et al., 2008), indicating that Dlk plays a fundamental role in development. Having identified Cfr as a Dlk-binding protein, we were interested in the functions of Cfr and the relation between Cfr and Dlk. To reveal the functions of Cfr, we generated *Cfr*-deficient mice and found that some of them die shortly after birth and show growth retardation, tail distortion and cleft palate. Among all the *Fgf*-deficient mice published, *Fgf18*-deficient mice were most similar to *Cfr*-deficient mice in terms of these

[1]Laboratory of Cell Growth and Differentiation, Institute of Molecular and Cellular Biosciences and [2]Promotion of Independence for Young Investigators, The University of Tokyo, Yayoi, Bunkyo-ku, Tokyo 113-0032, Japan. [3]Signaling Molecules Research Laboratory, National Institute of Advanced Industrial Science and Technology (AIST), Tsukuba, Ibaraki 305-8566, Japan. [4]Okazaki Institute for Integrative Biosciences, National Institutes of Natural Sciences, and [5]Department of Basic Biology, Graduate University for Advanced Studies (SOKENDAI), Okazaki, Aichi 444-8787, Japan.

*Author for correspondence (miyajima@iam.u-tokyo.ac.jp)

Accepted 21 October 2009

phenotypes (Liu et al., 2002; Ohbayashi et al., 2002). Fgf18 activates intracellular signaling mainly via Fgfr3c (Zhang et al., 2006), and it is well established that Fgf18-Fgfr3c signaling plays a central role in skeletal development (Haque et al., 2007). Fgf18 inhibits the proliferation of chondrocytes (Liu et al., 2002; Ohbayashi et al., 2002), and several Fgfr3 mutations in humans are known to be a cause of dwarfism (Horton et al., 2007). In this paper, we show genetic and physical interaction between Cfr and Fgf18, and a positive regulatory role of Cfr in Fgf18 signaling. Moreover, we also noticed that the phenotypes of *Cfr*-deficient mice are similar to those of *Dlk*-transgenic mice (Lee et al., 2003) and found that Dlk inhibits the physical interaction between Cfr and Fgf18. Taken together, these results imply that Dlk interferes with the positive regulatory role of Cfr in Fgf18 signaling by abrogating the binding between Cfr and Fgf18. Thus, our study reveals a novel regulatory mechanism for Fgf18 signaling involving Cfr and Dlk.

MATERIALS AND METHODS

Mice

Cfr-deficient mice were generated by using a gene-trapped 129Ola embryonic stem (ES) cell line (see Results). The cell line used for this research project, BayGenomics clone KST005 (catalog number 000716-UCD), was obtained from the Mutant Mouse Regional Resource Center (MMRRC), a NCRR-NIH funded strain repository, and was donated to the MMRRC by the NIH and NHLBI supported BayGenomics consortium. The mouse model will be made available (BRC No. RBRC03897) from the RIKEN BioResource Center (RIKEN BRC), which is participating in the National Bio-Resource Project of the MEXT, Japan, please contact them at animal@brc.riken.jp for inquiries, or search the catalog at http://www.brc.riken.go.jp/lab/animal/en/. The details of *Fgf18* targeting were described previously (Ohbayashi et al., 2002). The *Cfr*-mutant and *Fgf18*-mutant mice used in this study had been back crossed with C57BL/6 wild-type mice at least eight and ten times, respectively. All experimental procedures in this study were approved by the institutional animal care and use committee of the University of Tokyo.

Antibodies

The antibodies used were as follows: anti-Actin (sc-1616) purchased from Santa Cruz Biotechnology, rat monoclonal antibody against Dlk raised in our laboratory (Suzuki et al., 2008a); anti-Cfr rabbit serum raised against the N-terminal domain of Cfr without a signal sequence (28-256 amino acid residues), which was expressed in *Escherichia coli*, and anti-Fgf18 rabbit serum raised against full-length Fgf18 without a signal sequence, which was fused to a GST tag and expressed in *E. coli*.

Expression screening for Dlk-binding proteins

The extracellular domain of Dlk (1-303 amino acid residues) fused to the human IgG Fc region (Dlk-Fc) was expressed in COS7 cells and purified from the culture supernatant with a Hi Trap column (GE Healthcare), and then biotinylated with a biotinylation module (GE Healthcare) for flow cytometric analysis. First, we constructed a cDNA library of HPPL with the FastTrack 2.0 mRNA Isolation Kit (Invitrogen) and SuperScript Choice System (Invitrogen) in the pMXs retroviral vector. The plasmid was then converted to retrovirus using PLAT-E cells. Ba/F3 cells were infected with the virus library and Ba/F3 cells that bound Dlk-Fc were enriched by IMag (Becton Dickinson) cell sorting using biotinylated Dlk-Fc protein. Genomic PCR of the sorted cells revealed that some of them had the full-length *Cfr* sequence in their genomes (see Results).

Retroviral gene transfer and proliferation assay of Ba/F3 cells

We utilized a Ba/F3 cell line, which expresses a fusion protein of the extracellular domain of Fgfr3c and the intracellular domain of Fgfr1 described previously (Ornitz et al., 1996). For simplicity, we refer to this fusion protein as Fgfr3c in this report.

We constructed a pMXs-IRES-GFP vector encoding the full-length Cfr and produced retroviruses from the vector using PLAT-E cells as described previously (Miyaoka et al., 2006). Ba/F3 cells were infected with the viruses and cells expressing GFP were sorted by FACSVantage (Becton Dickinson).

For proliferation assay, Ba/F3 cells were deprived of cytokines for at least 6 hours, and then 2×10^3 Ba/F3 cells were cultured in 100 μl RPMI-1640 (SIGMA) containing 10% fetal bovine serum (EQUITECH-BIO), 2 mM L-glutamine, 50 μg/ml gentamicin (Wako), and the indicated reagents per 96 well for 2 or 3 days. We assessed the extent of proliferation by adding 10 μl WST-1 reagent (Roche) per 96 well, incubating at 37°C for 2 hours, and monitoring absorbance at 450 nm subtracted by basal absorbance at 650 nm. We set eight wells per one condition in all the experiments in this report.

Quantitative PCR analysis

For cDNA synthesis, total RNA was isolated with TRIzol Reagent (Invitrogen), and then reverse transcribed with a High Capacity cDNA Reverse Transcription Kit (Applied Biosystems). For analysis, SYBR Premix Ex Taq (Takara) and Light Cycler (Roche) were used.

Histochemistry

For immunohistochemistry, embryos were dissected and fixed with methanol/DMSO (4:1) at 4°C overnight, and then incubated in methanol/DMSO/H_2O_2 (4:1:1) at room temperature for 8 hours. Embryos were rehydrated and incubated with primary antibodies at 4°C overnight. They were then incubated with anti-rat IgG-HRP at 4°C overnight. Signal was visualized with 0.06% DAB/0.06% $NiCl_2$ in PBS with 0.2% BSA, 0.5% Triton X-100 and 0.03% H_2O_2.

For immunofluorescent staining, embryos were dissected and fixed with Zamboni's fixative at 4°C overnight, and then gradually substituted to 20% sucrose in PBS. The samples were sectioned and incubated with 5% skimmed milk in PBS for 2 hours at room temperature. They were then incubated with first antibodies at 4°C overnight, and with second antibody conjugated with Alexa Fluor 488 or 555 (Invitrogen) for 2 hours at room temperature. The sections were embedded with Gel/Mount (Cosmo Bio) containing Hoechst 33342.

For examining β-gal activity, embryos were dissected and fixed with 4% paraformaldehyde in PBS at room temperature for 10 minutes. After being washed with PBS, they were incubated in 1 mg/ml X-Gal, 5 mM ferricyanide, 5 mM ferrocyanide, 2 mM $MgCl_2$, 0.02% Nonidet-P 40 and 40 mM HEPES in PBS at 37°C for appropriate periods.

Western blot analysis and northern blot analysis

The detailed methods for western blot analysis and northern blot analysis were described previously (Miyaoka et al., 2006).

Alcian Blue/Alizarin Red staining of cartilage and bone

Mice were dissected, eviscerated, and fixed with 95% ethanol overnight. They were then incubated in acetone overnight. After a brief rinse with water, the samples were incubated in 20% acetate, 75% ethanol and 0.15 mg/ml Alcian Blue 8GX overnight. Then, the samples were washed with 70% ethanol for 8 hours, and cleared with 1% KOH overnight. For counterstaining, 0.05 mg/ml Alizarin Red in 1% KOH was used, and the samples were cleared in 1% KOH in 20% glycerol. All steps were done at room temperature.

Immunoprecipitation

The extracellular domain of Cfr (1-869 amino acid residues) fused tandemly to a His tag and a FLAG tag at its C-terminus (Cfr-EC) was expressed in COS7 cells and purified by using His Trap column (GE Healthcare). Protein G Sepharose (GE Healthcare) was used for precipitation of Fc-fused proteins. Cfr-EC was immunoprecipitated with anti-Cfr serum and protein G Sepharose, or anti-FLAG M2 agarose (SIGMA). These beads were incubated with culture supernatants or the lysis buffer (Miyaoka et al., 2006) containing their target proteins at 4°C for 4 hours, and then washed with the lysis buffer four times.

RESULTS

Identification of Cfr as a Dlk-binding molecule

First, we attempted to identify molecules that bind to Dlk by using an expression screening method. To find cells expressing Dlk-binding proteins on their surface, the extracelluar domain of Dlk

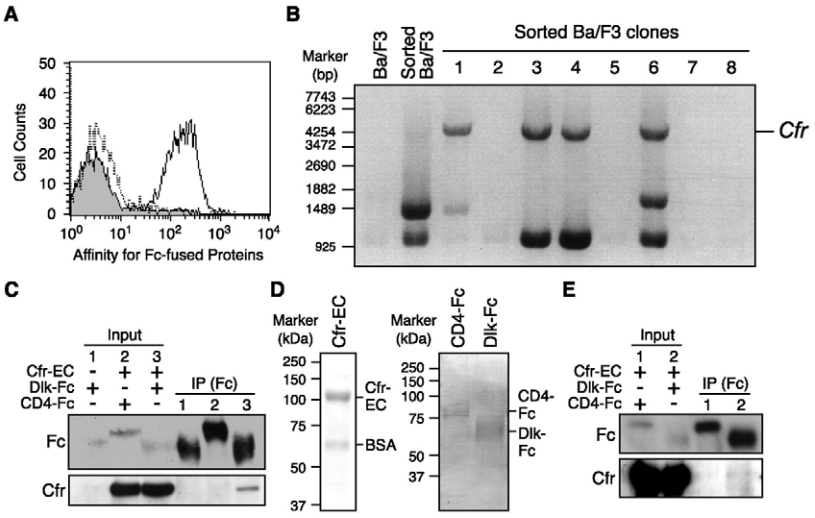

Fig. 1. Identification of Cfr as a Dlk-binding molecule. (**A**) Flow cytometric analysis of the binding of Dlk-Fc protein to HPPL. The specificity of the binding was confirmed with control CD4-Fc protein. Grey, no protein added; dotted line, CD4-Fc; unbroken line, Dlk-Fc. (**B**) DNA fragments inserted by retroviruses in Ba/F3 clones isolated by the cell sorting. Virus-sequence-specific primers amplified the inserted DNA fragments by PCR. Ba/F3, untreated Ba/F3 cells; sorted Ba/F3 cells, the sorted bulk Ba/F3 cells before cloning. (**C**) Immunoprecipitation confirming the binding between Dlk and Cfr. Plasmid constructs shown were introduced into COS7 cells, and Dlk-Fc or CD4-Fc was immunoprecipitated from the culture supernatants. Western blot analysis revealed that the extracellular domain of Cfr (Cfr-EC) was specifically co-immunoprecipitated with Dlk-Fc. (**D**) Coomassie Brilliant Blue staining of Cfr-EC, CD4-Fc and Dlk-Fc purified from COS7 culture supernatants. A weak signal of residual BSA was observed together with that of Cfr-EC. (**E**) Western blot analysis of the immunoprecipitates confirming the binding between the purified Dlk-Fc and Cfr-EC.

was fused to the Fc domain of human IgG (Dlk-Fc) and flow cytometry was used to find cells that bound Dlk-Fc. We found that Dlk-Fc strongly bound to HPPL, a hepatocyte progenitor cell line (Tanimizu et al., 2004) (Fig. 1A). To clone a cDNA encoding the Dlk-binding protein, a retroviral cDNA expression library was constructed from HPPL and introduced into Ba/F3 cells. Magnetic cell sorting was used to enrich Ba/F3 cells that bound Dlk-Fc. After three rounds of enrichment, we obtained several Ba/F3 clones that bound Dlk-Fc. Oligonucleotide primers specific for the retrovirus sequence were used to amplify the sequences introduced into the Ba/F3 genomes by the retrovirus. Sequencing of the amplified DNA fragments revealed that four of the eight clones contained in their genomes a full-length *Cfr* cDNA sequence (Fig. 1B). Other amplified DNA fragments seemed to be non-specific, because they were all truncated, not full-length fragments, and some of them were inserted in the reverse orientation to the retrovirus promoter (data not shown). As clones 1, 3 and 4, and 6 in Fig. 1B had different non-specific fragments inserted in the genomes, these clones were independently generated and acquired the affinity for Dlk-Fc by the *Cfr* insertion. We confirmed binding between Cfr and Dlk by immunoprecipitation. The extracellular domain of Cfr (Cfr-EC) was expressed in COS7 cells together with either Dlk-Fc or the extracellular domain of CD4 fused to the Fc domain of human IgG (CD4-Fc), and the Fc-fusion proteins were immunoprecipitated from the culture supernatants. As shown in Fig. 1C, Cfr-EC was co-precipitated with Dlk-Fc but not CD4-Fc. Then, we purified Cfr-EC, Dlk-Fc and CD4-Fc, and found that the purified Cfr-EC was also co-precipitated with the purified Dlk-Fc (Fig. 1D,E). These results indicate that Cfr directly interacts with Dlk. However, as the signal of the co-precipitated purified Cfr was relatively weak compared with that from the crude culture supernatants (Fig. 1C,E), it might be possible that the interaction is enhanced by other factors.

Generation of *Cfr*-deficient mice

As there has been no report on the physiological role of Cfr, we generated *Cfr*-deficient mice by utilizing a gene-trapped ES cell line. Because this ES cell line has a *β-geo* cassette with a splice acceptor inserted in the first intron of the *Cfr* locus, normal splicing between the first and second exons was interrupted, resulting in the production of a protein in which the peptide from the first exon is fused with β-geo (Fig. 2A). The ES cells were introduced into C57BL/6 blastocysts to generate chimeric mice, and a mouse with ES-cell-derived cells in its germline was obtained. First, we confirmed the site of the *β-geo* cassette in the first intron of the *Cfr* locus by inverse PCR (data not shown), and located it, in the correct orientation, about 10 kbp 3′ downstream from the end of the first exon (Fig. 2A). The insertion was further confirmed to be correct by PCR with primers indicated in Fig. 2A (Fig. 2B). To confirm the abrogation of Cfr protein expression, lysates from embryonic day 11.5 (E11.5) whole embryos of each genotype were subjected to a western blot analysis with antiserum raised against the N-terminal domain of Cfr. An embryo homozygous for the gene-trapped allele showed a protein larger than the wild-type Cfr, the molecular weight of which corresponds to that of a fusion protein comprising the peptide from the first exon of *Cfr* and β-geo. Both the intact Cfr and the fusion protein were detected in a heterozygous embryo (Fig. 2B). Because no intact Cfr protein was detected in the embryo homozygous for the gene-trapped allele, and the first exon of *Cfr* contains only its signal peptide with a few additional amino acid residues (117 amino acid residues), it is highly likely that the gene-trap results in a null mutation. Therefore, we refer to the gene-trapped allele as '–' hereafter. Mating between $Cfr^{+/-}$ mice resulted in the generation of embryos with the normal Mendelian segregation pattern until E18.5; however, about 90% of $Cfr^{-/-}$ mice died within 2 days after birth and there were only a few $Cfr^{-/-}$ mice alive at 3

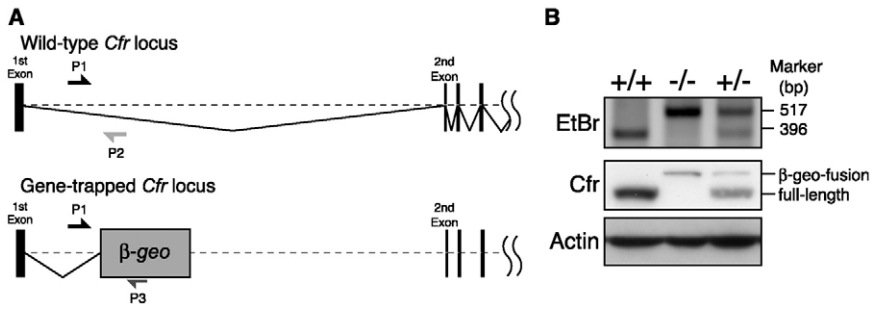

Fig. 2. Generation of *Cfr*-deficient mice. (**A**) Schematic representation of the wild-type and gene-trapped *Cfr* locus. The genomic region around the first intron is shown. In the trapped allele, a *β-geo* cassette is inserted in the first intron. To confirm the correct insertion, three oligonucleotide primers, P1-P3, were designed. (**B**) Confirmation of the gene-trapping. PCR with P1-P3 revealed that DNA fragments of the sizes expected from the genotypes were correctly amplified. The sizes of DNA fragments amplified with P1 and P2, and P1 and P3, should be 353 and 500 bp, respectively. The positions of DNA size markers are shown on the right. Western blot analysis of whole embryo lysate from each genotype with anti-Cfr serum revealed that the wild-type Cfr and the β-geo fusion proteins were expressed in the expected pattern from the wild-type allele and the trapped allele, respectively. No wild-type Cfr was detected in –/– embryos, indicating that this trapping resulted in a null mutation. The amount of protein loaded on the gel was confirmed by anti-actin blotting.

weeks of age (Table 1). Adult $Cfr^{-/-}$ mice had no obvious abnormality in their appearance, but their size and weight were significantly smaller than those of wild-type mice (data not shown). As a preliminary histological analysis of two $Cfr^{-/-}$ adult male survivors showed no obvious pathological abnormality in the brain, heart, lung, liver, spleen, kidney, stomach, guts, thymus, skin, skeletal muscle, eye or testis (data not shown), the cause of lethality is currently unknown. Because we identified Cfr as a Dlk-binding molecule, we considered the possibility that the lack of Cfr might affect the expression of Dlk. However, neither the mRNA nor protein level of Dlk was altered in *Cfr*-deficient mice (see Fig. S1A-D in the supplementary material). Because the inserted *β-geo* cassette expresses β-gal activity via the promoter of the inserted gene, the β-gal activity in $Cfr^{+/-}$ embryos represents the *Cfr* promoter activity. At E7.5, *Cfr* was expressed only in the epiblast, and thereafter ubiquitously at all stages examined, E8.5-14.5 (see Fig. S2A in the supplementary material and data not shown). Northern blot analysis using total RNA from various adult tissues revealed that *Cfr* was expressed in all the tissues examined, although levels were variable (see Fig. S2B in the supplementary material). Thus, Cfr is expressed broadly in the body from early embryonic stages to adulthood.

Growth retardation, skeletal abnormality and cleft palate in *Cfr*-deficient mice

At E18.5, $Cfr^{-/-}$ embryos were smaller in size and weighed less than $Cfr^{+/+}$ and $Cfr^{+/-}$ littermates (Fig. 3A,B). We also noticed that tails of all $Cfr^{-/-}$ E18.5 embryos and neonates were distorted, suggesting an abnormal skeletal development. In fact, Alcian Blue/Alizarin Red staining of bones and cartilages revealed that tail skeletons of $Cfr^{-/-}$ neonates were distorted, whereas the other skeletons were almost normal (Fig. 3C). The distortion seemed to be caused by an irregular arrangement of the tail cartilages (Fig. 3D). In addition, about 19% (7/37) of $Cfr^{-/-}$ neonates had a bloated abdomen filled with air (Fig. 3E). As cleft palate in mice often results in an accumulation of air in the stomach and a bloated abdomen, we investigated the palates of $Cfr^{-/-}$ neonates, and found that about 30% (11/37) of the mice exhibited cleft palate (Fig. 3F). All of the $Cfr^{-/-}$ mice with a bloated abdomen had a cleft palate. We investigated craniofacial skeletal elements and found incomplete fusion of maxillary shelves in $Cfr^{-/-}$ neonates with cleft palate (Fig. 3G). The other skeletal elements were apparently normal in $Cfr^{-/-}$ mice (Fig. 3C,G and data not shown). $Cfr^{+/-}$ mice showed no obvious abnormality. These results indicate that Cfr is essential for normal development.

Expression profile of Cfr and Dlk in developing skeletons

Although Cfr is ubiquitously expressed in embryos, as shown in Fig. S2 in the supplementary material, the skeletal abnormality of $Cfr^{-/-}$ mice prompted us to investigate more detailed expression patterns of Cfr in embryonic skeletons. We examined expression patterns of Cfr as well as Dlk in limbs, vertebrae and maxillae of E14.5 wild-type embryos by immunofluorescent staining and found that Cfr and Dlk were specifically expressed in prehypertrophic chondrocytes, and reserve and proliferating chondrocytes, respectively, in humeri (Fig. 4). The same expression patterns were observed in other limb skeletons (data not shown). Cfr and Dlk were also expressed in vertebrae and maxillae, although the specificity of cell-types or stages was unclear (see Fig. S3A,B in the supplementary material). Thus, Cfr and Dlk are expressed in developing skeletons, contributing to skeletal development.

Table 1. Genotypes of offspring from matings of $Cfr^{+/-}$ mice

	E9.5	E18.5	P0	P1	P2	3 week
+/+	26 (25.2)	32 (25.8)	40 (30.8)	32 (30.2)	76 (36.7)	63 (32.0)
+/–	51 (49.5)	57 (46.0)	70 (53.8)	69 (65.1)	124 (59.9)	129 (65.5)
–/–	26 (25.2)	35 (28.2)	20 (15.4)	5 (4.7)	7 (3.4)	5 (2.5)
Total	103	124	130	106	207	197

Male and female $Cfr^{+/-}$ mice were mated and genotypes of the offspring were analyzed at the indicated time points. The numbers in parentheses indicate the percentage of a genotype. The Mendelian segregation pattern was observed until E18.5, but the number of $Cfr^{-/-}$ mice was reduced after birth. By day 2 after birth, about 90% of $Cfr^{-/-}$ mice had died.

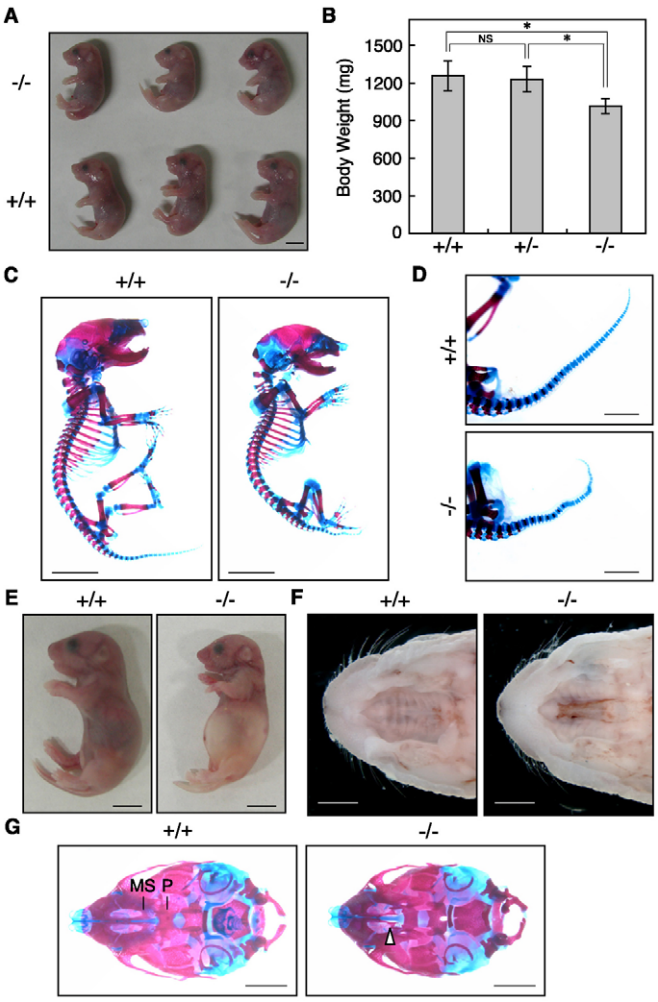

Fig. 3. Phenotypes of *Cfr*-deficient mice. (**A**) E18.5 $Cfr^{+/+}$ (lower three) and $Cfr^{-/-}$ (upper three) littermates. Note that the $Cfr^{-/-}$ embryos are smaller. (**B**) Body weight of E18.5 embryos with s.d. (+/+, *n*=25; +/–, *n*=46; –/–, *n*=30). *P*-value was calculated with Student's *t*-test: *, $P<0.001$; NS, $P>0.5$. (**C**) Alcian Blue/Alizarin Red staining of bone and cartilage of neonates. $Cfr^{-/-}$ neonates showed a basically normal skeleton except for their distorted tails. (**D**) Distorted tails of $Cfr^{-/-}$ neonates. All $Cfr^{-/-}$ neonates had a distorted tail. (**E**) Bloated abdomen of $Cfr^{-/-}$ neonates. About 19% (7/37) of $Cfr^{-/-}$ neonates had a bloated abdomen filled with air. (**F**) Cleft palate of $Cfr^{-/-}$ neonates. About 30% (11/37) of $Cfr^{-/-}$ neonates had a cleft palate. (**G**) Incomplete fusion of maxillary shelves in about 23% (3/13) of $Cfr^{-/-}$ neonates. Craniofacial skeletons were stained with Alcian Blue/Alizarin Red and viewed from beneath. For clarity, the lower jaws were removed. The arrowhead indicates the incomplete fusion of maxillary shelves. Scale bars: 2 mm in D,F,G; 5 mm in A,C,E. MS, maxillary shelves; P, palatine.

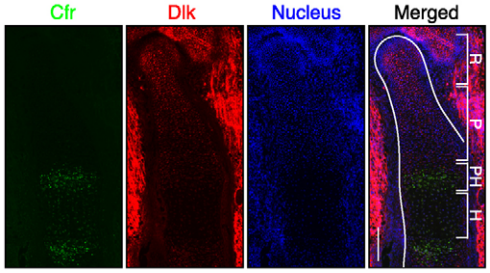

Fig. 4. Expression profiles of Cfr and Dlk in humeri. Immunofluorescent staining of Cfr (green) and Dlk (red) in E14.5 wild-type humeral longitudinal sections. In the merged photograph, the green and red signals are merged with signals of nuclei stained with Hoechst 33342 (blue), and humeri are outlined by a white line. Regions for reserve (R), proliferating (P), prehypertrophic (PH) and hypertrophic (H) chondrocytes are indicated. Note that Cfr is expressed specifically in prehypertrophic chondrocytes, while Dlk in reserve and proliferating chondrocytes. Scale bar: 80 μm.

Genetic interaction between *Cfr* and *Fgf18*

Because Cfr is an FGF-binding molecule, we considered that the observed phenotypes of *Cfr*-deficient mice were caused by deregulation of some of the FGF signaling pathways. To address this possibility, we compared *Cfr*-deficient mice with all the *Fgf*-deficient mice reported previously, and noticed that the phenotypes of $Cfr^{-/-}$ mice, such as perinatal death, growth retardation, tail distortion and cleft palate, are markedly similar to those of *Fgf18*-deficient mice. Therefore, we searched for a functional link between Cfr and Fgf18. First, we investigated whether there is any genetic interaction between *Cfr* and *Fgf18* by mating $Cfr^{+/-}$ mice with $Fgf18^{+/-}$ mice. Among the offspring, wild-type, $Cfr^{+/-}$ and $Fgf18^{+/-}$ mice had no obvious phenotype. $Cfr^{+/-};Fgf18^{+/-}$ double heterozygous (D-HT) mice were viable and fertile (data not shown). They were comparable in body weight to other genotypes and had a normal tail morphology at birth (see Fig. S4A,B in the supplementary material). However, D-HT mice were significantly smaller than wild-type mice at 3 months after birth, whereas neither $Cfr^{+/-}$ nor $Fgf18^{+/-}$ mice showed such a phenotype (Fig. 5A). The phenotype was more evident in D-HT male mice, as they were already smaller than wild-type male mice at 1 month after birth (Fig. 5A). Moreover, the tails of D-HT mice were distorted by 7 days after birth like those of *Cfr*-deficient mice and *Fgf18*-deficient mice, but neither $Cfr^{+/-}$ nor $Fgf18^{+/-}$ mice showed tail distortion (Fig. 5B,C). The tail distortion in D-HT mice was visible from postnatal day 3 and retained even in adulthood. About 83% (19/23) of adult D-HT mice showed the malformation. These phenotypes clearly indicate genetic interaction between *Cfr* and *Fgf18*, suggesting functional cooperation.

We further analyzed the genetic interaction between *Cfr* and *Fgf18* by crossing D-HT mice. As was the case for the offspring from mating of $Cfr^{+/-}$ mice (Table 1), some $Cfr^{-/-}$ neonates from mating of D-HT mice died after birth. Mortality among $Cfr^{-/-};Fgf18^{+/-}$ mice was similar to that among $Cfr^{-/-}$ mice, indicating that the lack of one *Fgf18* allele did not affect the viability of $Cfr^{-/-}$ mice (data not shown). Likewise, skeletons of $Cfr^{-/-}$ and $Cfr^{-/-};Fgf18^{+/-}$ neonates showed no significant difference (Fig. 5D). Consistent with the finding that the complete loss of *Fgf18* resulted in perinatal death and skeletal abnormalities (Liu et al., 2002; Ohbayashi et al., 2002), $Cfr^{+/-};Fgf18^{-/-}$, $Cfr^{-/-};Fgf18^{-/-}$ as well as $Fgf18^{-/-}$ mice died at birth. $Fgf18^{-/-}$ neonates showed slightly distorted ribs and the additional loss of one *Cfr* allele ($Cfr^{+/-};Fgf18^{-/-}$) enhanced the distortion of the ribs and caused curvature of the spine. In $Cfr^{-/-};Fgf18^{-/-}$ double knockout neonates, the distortion of the ribs and curvature of the spine were much more severe than in $Cfr^{+/-};Fgf18^{-/-}$ mice, although the number of ribs was normal and there was no fusion of the ribs (Fig. 5D). These results clearly indicate that Cfr and Fgf18 play indispensable and overlapping roles in skeletal development.

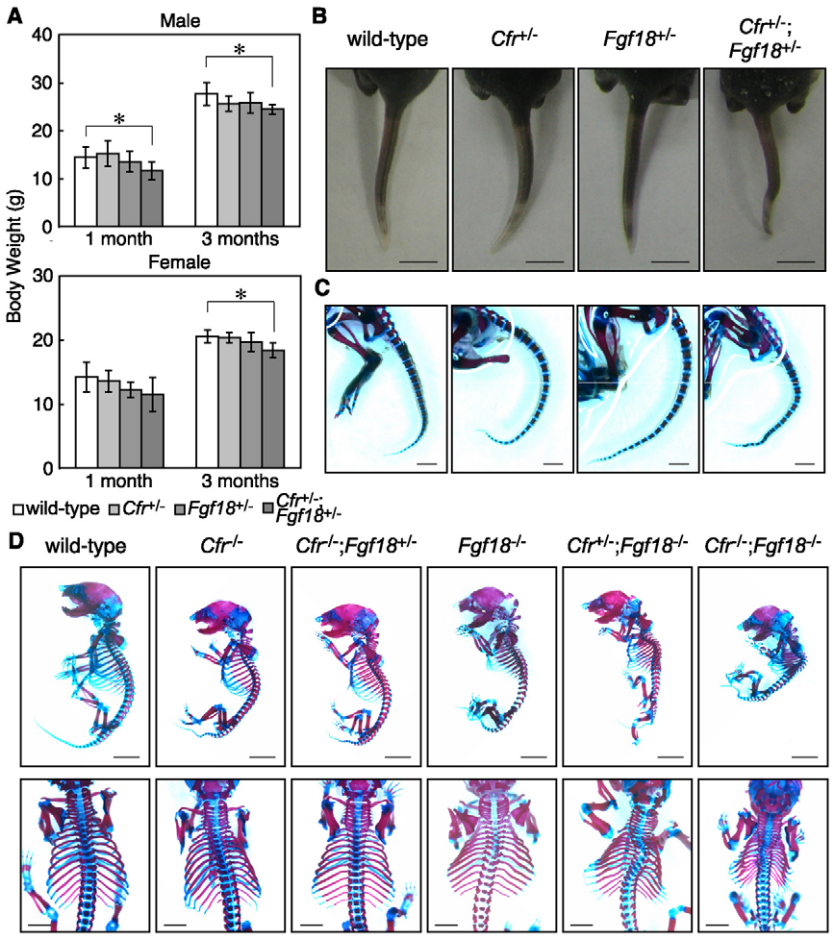

Fig. 5. Genetic interaction between *Cfr* and *Fgf18*. (**A**) Body weight of wild-type, $Cfr^{+/-}$, $Fgf18^{+/-}$ and $Cfr^{+/-}$;$Fgf18^{+/-}$ (double heterozygous, D-HT) 1 and 3 month(s) old mice from the mating of $Cfr^{+/-}$ and $Fgf18^{+/-}$ mice with s.d. (wild-type, *n*=6; $Cfr^{+/-}$, *n*=7; $Fgf18^{+/-}$, *n*=8; D-HT, *n*=6 for male) (wild type, *n*=5; $Cfr^{+/-}$, *n*=9; $Fgf18^{+/-}$, *n*=6; D-HT, *n*=9 for female). *P*-value was calculated with Student's *t*-test, *, $P<0.05$. Other *P*-values between wild-type mice and mutant mice are more than 0.07. (**B**) Tail morphology of wild-type, $Cfr^{+/-}$, $Fgf18^{+/-}$ and D-HT postnatal day 7 (P7) mice. D-HT mice developed distorted tails by P7, whereas the others had normal tails, indicating genetic interaction between *Cfr* and *Fgf18*. (**C**) Alcian Blue/Alizarin Red staining of the tails of P7 mice. Tail distortion in D-HT mice was evident, whereas tails were normal in other genotypes. (**D**) Skeletons of compound mutant neonates. $Cfr^{+/-}$;$Fgf18^{+/-}$ double heterozygotes were crossed to generate compound mutants. Skeletons of wild-type, $Cfr^{-/-}$, $Cfr^{-/-}$;$Fgf18^{+/-}$, $Fgf18^{-/-}$, $Cfr^{+/-}$;$Fgf18^{-/-}$ and $Cfr^{-/-}$;$Fgf18^{-/-}$ neonates were stained with Alcian Blue and Alizarin Red. Top row, whole skeletons; lower row, ribs and spines from behind. As in Fig. 3C,D, $Cfr^{-/-}$ neonates showed tail distortion, and $Cfr^{-/-}$;$Fgf18^{+/-}$ neonates showed no obvious difference from $Cfr^{-/-}$ neonates. $Fgf18^{-/-}$ neonates showed slight distortion of the ribs, and $Cfr^{+/-}$;$Fgf18^{-/-}$ neonates showed enhanced distortion of the tail and curvature of the spine. In $Cfr^{-/-}$;$Fgf18^{-/-}$ double knockout neonates, the distortion of the ribs and curvature of the spine were much more severe than in $Cfr^{+/-}$;$Fgf18^{-/-}$ neonates. Scale bars: 2 mm in C and top row in D; 4 mm in lower row in D; 5 mm in B.

Physical interaction between Cfr and Fgf18, and enhancement of Fgf18-Fgfr3c signaling by Cfr

We examined the possibility that the genetic interaction of *Cfr* with *Fgf18* resulted from their physical interaction. To address this possibility, we prepared recombinant Fgf18 protein with a GST tag (GST-Fgf18), and used the GST tag alone as a control (Fig. 7A). We also prepared culture supernatant of COS7 cells transfected with an expression vector for Cfr-EC. The purified GST-Fgf18 or GST tag was added to the supernatant, and Cfr-EC was immunoprecipitated. Western blot analysis revealed that GST-Fgf18 was co-immunoprecipitated with Cfr-EC, whereas the GST tag was not (Fig. 7B). These results clearly indicate that Fgf18 binds to Cfr and suggest that Cfr positively regulates Fgf18 signaling through this physical interaction.

To further confirm this possibility, we utilized a Ba/F3 cell line expressing Fgfr3c, which proliferates depending on Fgf18 (Ornitz et al., 1996). We chose Fgfr3c because it has the highest affinity for Fgf18 (Zhang et al., 2006) and is expressed in prehypertrophic chondrocytes in developing limb skeletons, where Cfr is also expressed (Ohbayashi et al., 2002) (Fig. 4). We infected these cells with viruses containing *Cfr* cDNA or without cDNA as a control, and assessed their responses to Fgf18 by WST-1 assay. Expression of Cfr enhanced the responses of Ba/F3 cells with Fgfr3c to Fgf18 (Fig. 6A), indicating that Cfr positively regulates Fgf18-Fgfr3c signaling. By contrast, Ba/F3 cells expressing Cfr alone failed to respond to Fgf18, whereas they proliferated in response to IL-3 (Fig. 6B). Based on these results, we concluded that Cfr enhances Fgf18 signaling via Fgfr3c but does not directly activate the intracellular signaling. As it is well known that heparin or HSPG is required for FGF signaling via FGFRs (Spivak-Kroizman et al., 1994; Yayon et al., 1991), we examined the effect of heparin on the Cfr function. We monitored responses of Ba/F3 cells expressing both Fgfr3c and Cfr to Fgf18 in the presence or absence of heparin and found that they failed to respond to Fgf18 at all in the absence of heparin, demonstrating that heparin is required for the function of Cfr (Fig. 6C).

Inhibition of the interaction between Cfr and Fgf18 by Dlk

The results described above demonstrate genetic, physical and functional interaction between Cfr and Fgf18. However, it still remained unknown how Dlk is involved in the interaction between Cfr and Fgf18.

As Cfr physically interacts with both Fgf18 and Dlk, we examined whether the binding of Dlk to Cfr affects the binding between Cfr and Fgf18. For this purpose, Cfr-EC was expressed in COS7 cells together with Dlk-Fc or CD4-Fc as a control. GST-Fgf18 fusion protein was then added to the culture supernatants and Cfr-EC was immunoprecipitated. Western blot analysis of the immunoprecipitates revealed that co-immunoprecipitation of Fgf18 with Cfr-EC was severely blocked in the presence of Dlk-Fc, but not CD4-Fc (Fig. 7C). These results indicate that Dlk interferes with the binding of Fgf18 to Cfr, resulting in interruption of the positive regulatory role of Cfr in Fgf18 signaling.

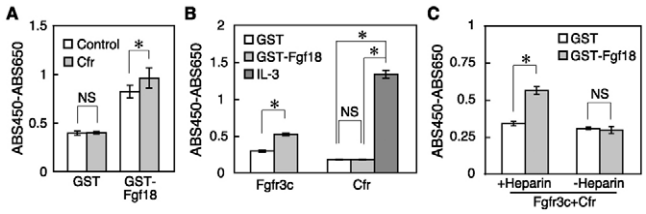

Fig. 6. Effects of Cfr in Fgf18 signaling in Ba/F3 cells. Ba/F3 cells were cultured in various conditions in 96 wells and the extent of proliferation was monitored by WST-1 assay. Absorbance at 450 nm subtracted by basal absorbance at 650 nm with s.d. is shown. We prepared eight wells for each condition. *P*-value was calculated with Student's *t*-test: *, $P<0.01$; NS, $P>0.2$. (**A**) Ba/F3 cells expressing Fgfr3c were infected with viruses carrying cDNA of *Cfr*, and we monitored proliferation in the presence of 500 ng/ml GST-Fgf18 or GST. As a control, Ba/F3 cells expressing Fgfr3c infected with viruses carrying no cDNA sequence were used. The cells with Cfr responded more strongly to Fgf18 than control cells. (**B**) Ba/F3 cells without FGFRs were infected with viruses carrying *Cfr* cDNA, and we monitored cell proliferation in the presence of 500 ng/ml GST-Fgf18 or GST, or 2 ng/ml IL-3. As a control for the activity of GST-Fgf18, we monitored responses of Ba/F3 cells with Fgfr3c to GST-Fgf18 at the same time. Ba/F3 cells with only Cfr could not respond to Fgf18, suggesting that Cfr does not directly activate the intracellular signaling pathways. (**C**) Ba/F3 cells with both Fgfr3c and Cfr were activated by 500 ng/ml GST-Fgf18 in the presence or absence of 5 μg/ml heparin. The same concentration of GST was added as a control. The cells could not respond to Fgf18 in the absence of heparin.

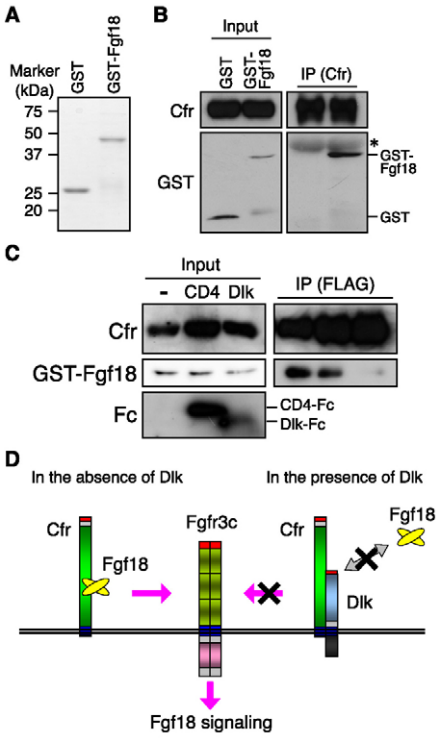

Fig. 7. The physical interaction between Cfr and Fgf18, and the effect of Dlk on that interaction. (**A**) Coomassie Brilliant Blue staining of GST and GST-Fgf18 purified from *E. coli*. (**B**) Interaction of Cfr with Fgf18. Cfr-EC was expressed in culture supernatant from COS7 cells, and GST-Fgf18 or GST was added to the supernatant. Then, Cfr-EC was precipitated with anti-Cfr serum and protein G Sepharose. GST-Fgf18, but not GST, was co-precipitated with Cfr-EC. *, non-specific band. (**C**) Interaction of Cfr with Fgf18 in the presence of Dlk. Cfr-EC together with Dlk-Fc or CD4-Fc were expressed in the culture supernatant from COS7 cells, and GST-Fgf18 was added to the supernatant. Then, FLAG-tagged Cfr-EC was precipitated with anti-FLAG M2 agarose. Dlk-Fc inhibited the interaction between Cfr and Fgf18, whereas CD4-Fc had no such effect. These results indicate that Dlk interrupts the physical interaction of Cfr with Fgf18. (**D**) A model of regulation of the Fgf18 signaling pathway by Cfr and Dlk. In the absence of Dlk, the extracellular domain of Cfr binds Fgf18 and positively regulates Fgf18 signaling. In the presence of Dlk, by contrast, Dlk binds to Cfr to inhibit the interaction between Cfr and Fgf18. Thus, the positive regulation of Fgf18 signaling by Cfr is disrupted by Dlk. Expression of Cfr and Dlk at the appropriate time modulates the strength of the signaling by Fgf18 and thereby contributes to normal developmental processes.

DISCUSSION

Cfr is a unique FGF-binding protein that binds FGFs via its long extracellular domain, but has a very short intracellular peptide of 13 amino acid residues without any known motifs for signaling. Therefore, it seems unlikely that Cfr directly activates the intracellular signaling pathways, which is in fact supported by the results using Ba/F3 cells expressing Cfr (Fig. 6B). Although Cfr seems to have no paralog in either mice or humans, it is evolutionally conserved and present even in *Caenorhabditis elegans* (data not shown), suggesting that Cfr is a fundamental component of the FGF signaling pathway. However, its physiological role remained unknown.

In this study we generated a *Cfr*-deficient mouse line and found that these mice exhibit perinatal lethality, growth retardation, distorted tails and cleft palates (Fig. 3). Another *Cfr*-deficient mouse line generated independently from this study shows the same phenotypes (H. Okae and Y. Iwakura, personal communication), supporting our results. Interestingly, among various *Fgf*-deficient mice reported so far, *Fgf18*-deficient mice exhibit phenotypes very similar to those of *Cfr*-deficient mice, such as perinatal death, growth retardation, tail distortion and cleft palate. Given this striking similarity, we considered that there is a functional link between Cfr and Fgf18. To address the genetic interaction of *Cfr* with *Fgf18*, double heterozygous mice were generated by mating $Cfr^{+/-}$ mice with $Fgf18^{+/-}$ mice. Although neither $Cfr^{+/-}$ nor $Fgf18^{+/-}$ mice showed any phenotype, the double heterozygous mice exhibited tail distortion after birth, suggesting genetic interaction (Fig. 5B,C). The phenotype is also strikingly similar to that of *Fgfr3*-deficient mice, which also exhibit tail distortion after birth (Deng et al., 1996). Because it has been well established that Fgf18 transmits its signal via Fgfr3c (Davidson et al., 2005), these observations further support the idea that Cfr is positively involved in Fgf18 signaling. Furthermore, co-immunoprecipitation assays clearly demonstrated that Cfr binds Fgf18 (Fig. 7B), and Ba/F3 cells expressing Fgfr3c with or without Cfr provided direct evidence for the positive regulatory role of Cfr in the Fgf18-Fgfr3c signaling pathway (Fig. 6A). This is the first report on the physiological functions of Cfr and the first evidence for the existence of a novel regulatory component of the Fgf18 signaling pathway. Fgfr3c is known to be expressed in proliferating and prehypertrophic chondrocytes to control their proliferation. Co-expression of Cfr with Fgfr3c in prehypertrophic chondrocytes supports the idea that Cfr plays a role in Fgfr3c signaling in those cells (Fig. 4). Because it has been well established that deregulation of the Fgf18-Fgfr3c signaling pathway leads to achondroplasia (Horton et al., 2007), it would be intriguing to investigate whether Cfr is also involved in human skeletal diseases.

Because Cfr has been shown to bind Fgf1, Fgf2, Fgf3 and Fgf4 (Burrus et al., 1992; Kohl et al., 2000), it may play a role in their signaling as well. In addition, the deletion of one *Cfr* allele in *Fgf18*-deficient mice augmented the skeletal abnormality of *Fgf18*-deficient mice and the deletion of both *Cfr* alleles in *Fgf18*-deficient mice resulted in a much more severe phenotype (Fig. 5D), suggesting that Cfr is involved in not only Fgf18 signaling but also other signaling pathways. However, as *Fgf4*-deficient mice die very early in their embryonic development (Feldman et al., 1995), and their phenotype is totally different from that of *Cfr*-deficient mice, Fgf4 is unlikely to be a physiological ligand for Cfr. By contrast, *Fgf3*-deficient mice show growth retardation and distorted tails, and some of them die perinatally similarly to *Cfr*-deficient mice, although their phenotypes are different from those of *Cfr*-deficient mice, e.g. inner ear defects in *Fgf3*-deficient mice (Mansour et al., 1993). Therefore, it is possible that Cfr contributes to Fgf3 signaling. Because *Fgf1*-deficient and *Fgf2*-deficient mice show rather mild phenotypes or no phenotype (Dono et al., 1998; Miller et al., 2000), it is hard to speculate about any possible involvement of Cfr in their signaling based on phenotypes. While there is currently no information as to the binding of Cfr to other FGFs, Cfr may contribute to signaling by some of them. In particular it would be interesting to investigate whether Cfr contributes to signaling by the FGFs that play a role in skeletal development, such as Fgf9 (Hung et al., 2007).

We identified Cfr as a Dlk-binding molecule (Fig. 1). Dlk is well known as preadipocyte factor 1 (Pref-1), an inhibitor of adipogenesis (Smas and Sul, 1993). In addition to preadipocytes, Dlk has also been reported to affect in vitro differentiation of various cell types such as osteoblasts (Abdallah et al., 2004), hematopoietic progenitors (Moore et al., 1997), thymocytes (Kaneta et al., 2000) and B-cell progenitors (Bauer et al., 1998). However, the mechanism by which Dlk functions still remains largely unknown. To reveal its functions, attempts were made to identify Dlk-binding molecules with the yeast two-hybrid system, resulting in several candidates such as growth arrest specific gene 1 (Baladron et al., 2002; Nueda et al., 2008). Because the extracellular domain of Dlk alone exerts its biological activities (Mei et al., 2002; Ohno et al., 2001; Smas et al., 1997), we used the extracellular domain of Dlk to search for its binding partners displayed on the cell surface and identified Cfr.

Because Dlk binds to Cfr, we investigated whether Dlk has any effect on the binding between Cfr and Fgf18 and revealed that Dlk blocks the binding (Fig. 7C). If the physical interaction of Cfr with Fgf18 is necessary for Cfr to positively regulate Fgf18 signaling, Dlk is likely to abrogate the positive role of Cfr in the signaling. We noticed that the phenotypes of *Cfr*-deficient mice are similar to those of *Dlk*-transgenic mice: e.g. both mice show growth retardation throughout their life and tail distortion (Lee et al., 2003). As loss of *Cfr* and forced expression of *Dlk* resulted in similar phenotypes, it is likely that Cfr and Dlk function in opposite ways. This is consistent with the result that Dlk inhibits the physical interaction between Cfr and Fgf18. Based on these results, we propose a model for the roles of Cfr and Dlk in Fgf18 signaling (Fig. 7D): i.e. in the absence of Dlk, binding of Cfr to Fgf18 positively regulates the signaling, and Dlk blocks the interaction between Cfr and Fgf18 by binding to Cfr, interrupting the positive regulatory role of Cfr in Fgf18 signaling. If this model is correct, the levels and timing of the expression of Cfr and Dlk would modulate Fgf18 signaling, fulfilling normal developmental processes. Recently, it was reported that Dlk regulates mesenchymal cell fate, such as chondrocyte, osteoblast and adipocyte lineages, through Sox9 (Wang and Sul, 2009). It is well known that Fgf18 also regulates chondrocyte and osteoblast development. Therefore, it is tempting to speculate that Fgf18 signaling is involved in the mechanism of cell-fate determination.

Recent studies have revealed that the FGF signaling via FGFRs is finely tuned by FGF-binding molecules other than FGFRs, such as HSPGs, Klothos and Fgfrl1 (Kurosu et al., 2007; Kurosu et al., 2006; Spivak-Kroizman et al., 1994; Suzuki et al., 2008b; Trueb et al., 2003; Urakawa et al., 2006). These molecules significantly contribute to normal developmental processes mediated by the FGF signaling pathways. This study has revealed, for the first time, in vivo roles of another FGF-binding molecule, Cfr, and unexpected links among Dlk, Cfr and FGF signaling, and provides evidence for the presence of a novel regulatory mechanism of the FGF signaling pathway.

Acknowledgements

We thank Drs T. Itoh, N. Tanimizu and E. Saijou, and Mr S. Saito for helpful discussions and technical assistance. We thank Ms K. Suzuki for preparing anti-Dlk antibody. We are also grateful to Drs A. Nakano, H. Okae, Y. Iwakura (the University of Tokyo), N. Mizushima, Y. Ogawa (Tokyo Medical and Dental University), J. Kanno, S. Kitajima, Y. Takahashi (National Institute of Health Science), N. Ohbayashi (Tohoku University) and T. Okubo (Okazaki Institute for Integrative Biosciences) for helpful advice and support. We thank Drs D. M. Ornitz (Washington University) and N. Itoh (Kyoto University) for providing us with cDNAs of FGFRs and Fgf18, respectively. Y.M. is a recipient of a JSPS Research Fellowship for Young Scientists.

Supplementary material

Supplementary material for this article is available at
http://dev.biologists.org/lookup/suppl/doi:10.1242/dev.041574/-/DC1

References

Abdallah, B. M., Jensen, C. H., Gutierrez, G., Leslie, R. G., Jensen, T. G. and Kassem, M. (2004). Regulation of human skeletal stem cells differentiation by Dlk1/Pref-1. *J. Bone Miner. Res.* **19**, 841-852.

Baertschi, S., Zhuang, L. and Trueb, B. (2007). Mice with a targeted disruption of the Fgfrl1 gene die at birth due to alterations in the diaphragm. *FEBS J.* **274**, 6241-6253.

Baladron, V., Ruiz-Hidalgo, M. J., Bonvini, E., Gubina, E., Notario, V. and Laborda, J. (2002). The EGF-like homeotic protein dlk affects cell growth and interacts with growth-modulating molecules in the yeast two-hybrid system. *Biochem. Biophys. Res. Commun.* **291**, 193-204.

Bauer, S. R., Ruiz-Hidalgo, M. J., Rudikoff, E. K., Goldstein, J. and Laborda, J. (1998). Modulated expression of the epidermal growth factor-like homeotic protein dlk influences stromal-cell-pre-B-cell interactions, stromal cell adipogenesis, and pre-B-cell interleukin-7 requirements. *Mol. Cell. Biol.* **18**, 5247-5255.

Burrus, L. W. and Olwin, B. B. (1989). Isolation of a receptor for acidic and basic fibroblast growth factor from embryonic chick. *J. Biol. Chem.* **264**, 18647-18653.

Burrus, L. W., Zuber, M. E., Lueddecke, B. A. and Olwin, B. B. (1992). Identification of a cysteine-rich receptor for fibroblast growth factors. *Mol. Cell. Biol.* **12**, 5600-5609.

Davidson, D., Blanc, A., Filion, D., Wang, H., Plut, P., Pfeffer, G., Buschmann, M. D. and Henderson, J. E. (2005). Fibroblast growth factor (FGF) 18 signals through FGF receptor 3 to promote chondrogenesis. *J. Biol. Chem.* **280**, 20509-20515.

Deng, C., Wynshaw-Boris, A., Zhou, F., Kuo, A. and Leder, P. (1996). Fibroblast growth factor receptor 3 is a negative regulator of bone growth. *Cell* **84**, 911-921.

Dono, R., Texido, G., Dussel, R., Ehmke, H. and Zeller, R. (1998). Impaired cerebral cortex development and blood pressure regulation in FGF-2-deficient mice. *EMBO J.* **17**, 4213-4225.

Eswarakumar, V. P., Lax, I. and Schlessinger, J. (2005). Cellular signaling by fibroblast growth factor receptors. *Cytokine Growth Factor Rev.* **16**, 139-149.

Feldman, B., Poueymirou, W., Papaioannou, V. E., DeChiara, T. M. and Goldfarb, M. (1995). Requirement of FGF-4 for postimplantation mouse development. *Science* **267**, 246-249.

Haque, T., Nakada, S. and Hamdy, R. C. (2007). A review of FGF18: its expression, signaling pathways and possible functions during embryogenesis and post-natal development. *Histol. Histopathol.* **22**, 97-105.

Horton, W. A., Hall, J. G. and Hecht, J. T. (2007). Achondroplasia. *Lancet* **370**, 162-172.

Hung, I. H., Yu, K., Lavine, K. J. and Ornitz, D. M. (2007). FGF9 regulates early hypertrophic chondrocyte differentiation and skeletal vascularization in the developing stylopod. *Dev. Biol.* **307**, 300-313.
Kaneta, M., Osawa, M., Sudo, K., Nakauchi, H., Farr, A. G. and Takahama, Y. (2000). A role for pref-1 and HES-1 in thymocyte development. *J. Immunol.* **164**, 256-264.
Kohl, R., Antoine, M., Olwin, B. B., Dickson, C. and Kiefer, P. (2000). Cysteine-rich fibroblast growth factor receptor alters secretion and intracellular routing of fibroblast growth factor 3. *J. Biol. Chem.* **275**, 15741-15748.
Kurosu, H., Ogawa, Y., Miyoshi, M., Yamamoto, M., Nandi, A., Rosenblatt, K. P., Baum, M. G., Schiavi, S., Hu, M. C., Moe, O. W. et al. (2006). Regulation of fibroblast growth factor-23 signaling by klotho. *J. Biol. Chem.* **281**, 6120-6123.
Kurosu, H., Choi, M., Ogawa, Y., Dickson, A. S., Goetz, R., Eliseenkova, A. V., Mohammadi, M., Rosenblatt, K. P., Kliewer, S. A. and Kuro-o, M. (2007). Tissue-specific expression of betaKlotho and fibroblast growth factor (FGF) receptor isoforms determines metabolic activity of FGF19 and FGF21. *J. Biol. Chem.* **282**, 26687-26695.
Lee, K., Villena, J. A., Moon, Y. S., Kim, K. H., Lee, S., Kang, C. and Sul, H. S. (2003). Inhibition of adipogenesis and development of glucose intolerance by soluble preadipocyte factor-1 (Pref-1). *J. Clin. Invest.* **111**, 453-461.
Liu, Z., Xu, J., Colvin, J. S. and Ornitz, D. M. (2002). Coordination of chondrogenesis and osteogenesis by fibroblast growth factor 18. *Genes Dev.* **16**, 859-869.
Mansour, S. L., Goddard, J. M. and Capecchi, M. R. (1993). Mice homozygous for a targeted disruption of the proto-oncogene int-2 have developmental defects in the tail and inner ear. *Development* **117**, 13-28.
Mei, B., Zhao, L., Chen, L. and Sul, H. S. (2002). Only the large soluble form of preadipocyte factor-1 (Pref-1), but not the small soluble and membrane forms, inhibits adipocyte differentiation: role of alternative splicing. *Biochem. J.* **364**, 137-144.
Miller, D. L., Ortega, S., Bashayan, O., Basch, R. and Basilico, C. (2000). Compensation by fibroblast growth factor 1 (FGF1) does not account for the mild phenotypic defects observed in FGF2 null mice. *Mol. Cell. Biol.* **20**, 2260-2268.
Miyaoka, Y., Tanaka, M., Naiki, T. and Miyajima, A. (2006). Oncostatin M inhibits adipogenesis through the RAS/ERK and STAT5 signaling pathways. *J. Biol. Chem.* **281**, 37913-37920.
Moon, Y. S., Smas, C. M., Lee, K., Villena, J. A., Kim, K. H., Yun, E. J. and Sul, H. S. (2002). Mice lacking paternally expressed Pref-1/Dlk1 display growth retardation and accelerated adiposity. *Mol. Cell. Biol.* **22**, 5585-5592.
Moore, K. A., Pytowski, B., Witte, L., Hicklin, D. and Lemischka, I. R. (1997). Hematopoietic activity of a stromal cell transmembrane protein containing epidermal growth factor-like repeat motifs. *Proc. Natl. Acad. Sci. USA* **94**, 4011-4016.
Nueda, M. L., Garcia-Ramirez, J. J., Laborda, J. and Baladron, V. (2008). dlk1 specifically interacts with insulin-like growth factor binding protein 1 to modulate adipogenesis of 3T3-L1 cells. *J. Mol. Biol.* **379**, 428-442.
Ohbayashi, N., Shibayama, M., Kurotaki, Y., Imanishi, M., Fujimori, T., Itoh, N. and Takada, S. (2002). FGF18 is required for normal cell proliferation and differentiation during osteogenesis and chondrogenesis. *Genes Dev.* **16**, 870-879.
Ohno, N., Izawa, A., Hattori, M., Kageyama, R. and Sudo, T. (2001). dlk inhibits stem cell factor-induced colony formation of murine hematopoietic progenitors: Hes-1-independent effect. *Stem Cells* **19**, 71-79.
Ornitz, D. M., Xu, J., Colvin, J. S., McEwen, D. G., MacArthur, C. A., Coulier, F., Gao, G. and Goldfarb, M. (1996). Receptor specificity of the fibroblast growth factor family. *J. Biol. Chem.* **271**, 15292-15297.
Raghunandan, R., Ruiz-Hidalgo, M., Jia, Y., Ettinger, R., Rudikoff, E., Riggins, P., Farnsworth, R., Tesfaye, A., Laborda, J. and Bauer, S. R. (2008). Dlk1 influences differentiation and function of B lymphocytes. *Stem Cells Dev.* **17**, 495-507.
Smas, C. M. and Sul, H. S. (1993). Pref-1, a protein containing EGF-like repeats, inhibits adipocyte differentiation. *Cell* **73**, 725-734.
Smas, C. M., Chen, L. and Sul, H. S. (1997). Cleavage of membrane-associated pref-1 generates a soluble inhibitor of adipocyte differentiation. *Mol. Cell. Biol.* **17**, 977-988.
Spivak-Kroizman, T., Lemmon, M. A., Dikic, I., Ladbury, J. E., Pinchasi, D., Huang, J., Jaye, M., Crumley, G., Schlessinger, J. and Lax, I. (1994). Heparin-induced oligomerization of FGF molecules is responsible for FGF receptor dimerization, activation, and cell proliferation. *Cell* **79**, 1015-1024.
Suzuki, K., Tanaka, M., Watanabe, N., Saito, S., Nonaka, H. and Miyajima, A. (2008a). p75 Neurotrophin receptor is a marker for precursors of stellate cells and portal fibroblasts in mouse fetal liver. *Gastroenterology* **135**, 270-281 e3.
Suzuki, M., Uehara, Y., Motomura-Matsuzaka, K., Oki, J., Koyama, Y., Kimura, M., Asada, M., Komi-Kuramochi, A., Oka, S. and Imamura, T. (2008b). betaKlotho is required for fibroblast growth factor (FGF) 21 signaling through FGF receptor (FGFR) 1c and FGFR3c. *Mol. Endocrinol.* **22**, 1006-1014.
Tanimizu, N., Nishikawa, M., Saito, H., Tsujimura, T. and Miyajima, A. (2003). Isolation of hepatoblasts based on the expression of Dlk/Pref-1. *J. Cell Sci.* **116**, 1775-1786.
Tanimizu, N., Saito, H., Mostov, K. and Miyajima, A. (2004). Long-term culture of hepatic progenitors derived from mouse Dlk+ hepatoblasts. *J. Cell Sci.* **117**, 6425-6434.
Trueb, B., Zhuang, L., Taeschler, S. and Wiedemann, M. (2003). Characterization of FGFRL1, a novel fibroblast growth factor (FGF) receptor preferentially expressed in skeletal tissues. *J. Biol. Chem.* **278**, 33857-33865.
Urakawa, I., Yamazaki, Y., Shimada, T., Iijima, K., Hasegawa, H., Okawa, K., Fujita, T., Fukumoto, S. and Yamashita, T. (2006). Klotho converts canonical FGF receptor into a specific receptor for FGF23. *Nature* **444**, 770-774.
Wang, Y. and Sul, H. S. (2009). Pref-1 regulates mesenchymal cell commitment and differentiation through Sox9. *Cell Metab.* **9**, 287-302.
Wiedemann, M. and Trueb, B. (2000). Characterization of a novel protein (FGFRL1) from human cartilage related to FGF receptors. *Genomics* **69**, 275-279.
Yayon, A., Klagsbrun, M., Esko, J. D., Leder, P. and Ornitz, D. M. (1991). Cell surface, heparin-like molecules are required for binding of basic fibroblast growth factor to its high affinity receptor. *Cell* **64**, 841-848.
Zhang, X., Ibrahimi, O. A., Olsen, S. K., Umemori, H., Mohammadi, M. and Ornitz, D. M. (2006). Receptor specificity of the fibroblast growth factor family: the complete mammalian FGF family. *J. Biol. Chem.* **281**, 15694-15700.
Zhou, Z., Zuber, M. E., Burrus, L. W. and Olwin, B. B. (1997). Identification and characterization of a fibroblast growth factor (FGF) binding domain in the cysteine-rich FGF receptor. *J. Biol. Chem.* **272**, 5167-5174.